Published in final edited form as:
Gastroenterology. 2012 September ; 143(3): 787–798.e13. doi:10.1053/j.gastro.2012.05.050.

Hepatoma Cells from Mice Deficient in Glycine N-Methyltransferase Have Increased RAS Signaling and Activation of Liver Kinase B1

Nuria Martínez-López[1,†], **Juan L García-Rodríguez**[1,†], **Marta Varela-Rey**[1], **Virginia Gutiérrez**[1], **David Fernández-Ramos**[1], **Naiara Beraza**[1], **Ana M Aransay**[1], **Karin Schlangen**[1], **Juan Jose Lozano**[2], **Patricia Aspichueta**[3], **Zigmund Luka**[4], **Conrad Wagner**[4], **Matthias Evert**[5], **Diego F Calvisi**[5], **Shelly C Lu**[6], **José M Mato**[1], and **María L Martínez-Chantar**[1]

[1]CIC bioGUNE, Centro de Investigación Biomédica en Red de Enfermedades Hepáticas y Digestivas (Ciberehd), Technology Park of Bizkaia, 48160-Derio, Bizkaia, Spain

[2]Centro de Investigación Biomédica en red de Enfermedades Hepáticas y Digestivas (CIBEREHD), Hospital Clinic, Centre Esther Koplovitz (CEK), C/ Rosselló 153, 08036-Barcelona, Spain

[3]Department of Physiology, University of the Basque Country Medical School, Bilbao, Spain

[4]Department of Biochemistry, Vanderbilt University Medical Center, Nashville, Teennesse, 37232, USA

[5]Institute of Pathology, Ernst-Moritz-Arndt-Universität Greifswald, Germany

Corresponding author: ML Martínez-Chantar, CIC bioGUNE, Technology Park of Bizkaia, 48160 Derio, Bizkaia, Spain. mlmartinez@cicbiogune.es; **Tel**: +34-944-061318; **Fax**: +34-944-061301..
[†]NM-L and JLG-R contributed equally to this paper.

Conflict of interest: The authors have declared that no conflict of interest exists.

Transcript Profiling-Provide accession number of repository for expression microarray data. Experiment name: RAS-dependent LKB1 hyperactivation in GNMT-deficient hepatocellular carcinoma. Array Express accession: E-MEXP-3403.

Author Contributions Nuria Martínez-López; Study concept and design; acquisition of data; analysis and interpretation of data; critical revision of the manuscript.
Juan L García-Rodríguez; Study concept and design; acquisition of data; analysis and interpretation of data; critical revision of the manuscript.
Marta Varela-Rey; Study concept and design; acquisition of data; analysis and interpretation of data; critical revision of the manuscript.
Virginia Gutiérrez; Acquisition of data.
David Fernández-Ramos; Acquisition of data.
Naiara Beraza; Acquisition of data.
Ana M Aransay; Acquisition of data.
Karin Schlangen; Acquisition of data.
Juan Jose Lozano; Acquisition of data.
Patricia Aspichueta; Acquisition of data.
Zigmund Luka; Material Provided.
Conrad Wagner; Material Provided.
Matthias Evert; Acquisition of data.
Diego F Calvisi; Acquisition of data; analysis and interpretation of data.
Shelly C Lu; Obtained funding; critical revision of the manuscript.
José M Mato; Obtained funding; material provided; critical revision of the manuscript.
María L Martínez-Chantar; Writing the manuscript; study concept and design; analysis and interpretation of data; obtained funding.

[6]Division of Gastrointestinal and Liver Diseases, USC Research Center for Liver Diseases, Southern California Research Center for Alcoholic Liver and Pancreatic Diseases and Cirrhosis, Keck School of Medicine, University of Southern California, Los Angeles, CA 90033

Abstract

Background & Aims—Patients with cirrhosis are at high risk for developing hepatocellular carcinoma (HCC), and their liver tissues have abnormal levels of adenosylmethionine (SAMe). Glycine N-methyltransferase (GNMT) catabolizes SAMe but its expression is downregulated in HCC cells. Mice that lack GNMT develop fibrosis and hepatomas and have alterations in signaling pathways involved in carcinogenesis. We investigated the role of GNMT in human HCC cell lines and in liver carcinogenesis in mice.

Methods—We studied hepatoma cells from GNMT knockout mice and analyzed the roles of liver kinase B1 (LKB1, STK11) signaling via 5'-AMP-activated protein kinase (AMPK) and Ras in regulating proliferation and transformation.

Results—Hepatoma cells from GNMT mice had defects in LKB1 signaling to AMPK, making them resistant to induction of apoptosis by cAMP activation of protein kinase A and calcium/calmodulin-dependent protein kinase kinase-2. Ras-mediated hyperactivation of LKB1 promoted proliferation of GNMT-deficient hepatoma cells, and required mitogen-activated protein kinase-2 (ERK) and ribosomal protein S6 kinase polypeptide-2 (p90RSK).

Ras activation of LKB1 required expression of RAS guanyl releasing protein-3 (RASGRP3). Reduced levels of GNMT and phosphorylation of AMPKα at Thr172 and increased levels of Ras, LKB1, and RASGRP3 in HCC samples from patients were associated with shorter survival times.

Conclusions—Reduced expression of GNMT in mouse hepatoma cells and human HCC cells appears to increase activity of LKB1 and RAS; activation of RAS signaling to LKB1 and RASGRP3, via ERK and p90RSK, might be involved in liver carcinogenesis and be used as a prognostic marker. Reagents that disrupt this pathway might be developed to treat patients with HCC.

Keywords

CAMKK2; AMP; liver cancer; mouse model

Introduction

Hepatocellular carcinoma (HCC) is the third cause of cancer death globally and the leading cause of death in cirrhotic patients (1).

Patients with liver cirrhosis at a high risk of HCC have impaired methionine metabolism and abnormal S-adenosylmethionine (SAMe) levels (2). SAMe, the main cellular methyl donor, is critical in cell proliferation, differentiation and apoptosis (3). MAT (methionine adenosyltransferase) and GNMT (glycine N-methyltransferase) catalyze the synthesis and catabolism of SAMe, respectively. Deficiency in GNMT has been reported in human HCC and GNMT-KO mice, and it is characterized by an increased in hepatic SAMe content, liver steatosis, fibrosis, and HCC. Results from our laboratory indicate that HCC development in GNMT-KO mice is mediated by epigenetic mechanism due to DNA hypermethylation (4–6).

Aberrant Ras/MEK/ERK pathway contributes to the malignant phenotype in cancer (7,8). In melanoma, a specific mutation in $BRAF^{V600E}$ induces a constitutive hyperactivation of ERK1/2-p90RSK-LKB1 pathway uncoupling LKB1-mediated AMPK activation and

providing growth advantage to tumor cells (9,10). In the liver, the metabolic tumor suppressor LKB1 has been reported to play a role in proliferation and regeneration (11). Moreover, we found that LKB1 is essential for liver tumor proliferation in MAT1A-KO mice, regulating AKT-mediated survival independent of PI3K, AMPK, and mTORC2 (12). More importantly, hyper-phosphorylation of LKB1(Ser428) has been associated to human HCC derived from NAFLD.

In the present work, we have isolated a hepatoma cell line derived from GNMT-KO mice liver tumors (OKER cells) to study the molecular mechanisms responsible for GNMT-deficient HCC. Our data indicate that hyper-phosphorylation of LKB1(Ser428) is critical for HCC survival in conditions where the expression of *GNMT* is compromised. Furthermore, GNMT chronic deficiency, and the consequent SAMe excess, hyperactivate Ras due to epigenetic silencing of *RASSF1A*, a Ras inhibitor. We also showed that non-mutated Ras pathway is responsible for the ERK/p90RSK-mediated LKB1 hyper-phosphorylation(Ser428), leading to LKB1-AMPK misconnection. Treatment with the demethylating agent, 5′-azacytidine, abolished the Ras pathway, induced CAMKKβ-mediated AMPK activation and promoted apoptosis. Also, LKB1 ablation triggered apoptosis. In a xenograft model in nude mice, LKB1 suppression decreased tumor growth, induced necrosis, AMPK activation and dramatically reduced Ras activity, the latter due to the decrease in RASGRP3, a Ras activator.

Moreover, statistical association between decreased *GNMT* levels and upregulation of *RASGRP3* gene was identified in 225 HCC human samples. Finally, a correlation between the *GNMT* expression levels and the expression of the LKB1 gene *STK11*, p-LKB1(Ser428), p-AMPKα(Thr172), and Ras-GTP activity and the poorest prognosis of HCC patients has been established.

In summary, we identified a novel crosstalk between LKB1 and Ras in a tumor environment with no *GNMT* expression, unveiling a novel-signaling paradigm pharmacologically amenable for HCC therapy.

Results

Characterization of the OKER cell line

OKER cells were isolated from the HCC of GNMT-KO mice. A detailed description of the procedure is provided in Supplemental Material and Methods. Gene expression arrays of OKER cells compared with WT hepatocytes, showed increased expression of TGF-β pathway, cell cycle and ribosomal proteins, and pancreatic cancer markers in OKER cells compared to WT hepatocytes (Suppl. .1). The differentially expressed-genes resulting of the microarray analysis are supplied in Suppl Tables M1, M2 and M3.

OKER cells fail to express *MAT1A* and *GNMT* genes (Fig.1A). Hence, this cell line and GNMT-KO hepatocytes are characterized by higher levels of SAMe than WT hepatocytes (Fig.1B) (6). Ras and Jak/STATs pathways hyperactivation has been described in livers from GNMT-KO mice due to epigenetic silencing of their major inhibitors, *RASSF1A* and *SOCS1* (6). In OKER and GNMT-KO hepatocytes compared with WT mouse hepatocytes, we observed an abnormally decreased expression of the *SOCS*, and *RASSF* inhibitors that correlated in OKER cells with *HRAS* and *NRAS* overexpression (Fig.1C), suggesting hyperactivation of the Ras pathway.

Mutations in *RAS* and in the Ras effector *BRAF* have been reported in cancers with hyperactivated Ras cascade. Similar to that observed in human HCC, no mutations in codon 12, 13 or 61 in the three isoforms of *RAS* or $BRAF^{V600E}$ were detected in OKER cells

(Suppl. Table 1). We found increased levels of p-ERK(Thr202/Tyr204), its target p-p90RSK(Thr359/Ser363) and antiapoptotic markers in OKER vs. WT hepatocytes (Fig.1E), while GNMT-KO hepatocytes displayed a mixed phenotype. Despite the levels of p-LKB1(Ser428) were highly increased in OKER cells, a hypo-phosphorylation of the LKB1 downstream kinase AMPKα(Thr172) occurred, suggesting an alternative pathway regulating AMPK in these cells (Fig.1E).

The Ras/MEK/ERK pathway regulates p-LKB1(Ser428)

The Ras/MEK/ERK cascade plays a pivotal role in cell growth and survival during hepatocarcinogenesis in GNMT-KO mice (6). Sorafenib, a Raf serine/threonine inhibitor, has been approved for clinical treatment of HCC and renal cell carcinoma (8, 13). In OKER cells, Sorafenib decreased p-ERK(Thr202/Tyr204), p-p90RSK(Thr359/Ser363), p-LKB1(Ser428) and induced p-AMPKα(Thr172) together with PARP cleavage (Fig.2A), supporting the Ras cascade in the regulation of LKB1 phosphorylation and the apoptotic response in this cell line.

Recent studies in melanoma cells demonstrated enhanced association between LKB1 and ERK in cells harboring mutant $BRAF^{V600E}$ (9. 10). Although OKER cells did not harbor mutations either in $BRAF^{V600E}$ gene or in the LKB1 gene (Suppl. Table 1), the inhibition of MEK/ERK signaling with U0126 tstrongly decreased p-LKB1(Ser428), completely inhibited p-ERK(Thr202/tyr204) and p-p90RSK(Thr359/Ser363) and activated p-AMPKα(Thr172) accordingly with the PARP cleavage (Fig.2B). Although immunoprecipitation assays did not detect a BRAF-LKB1 interaction (data not shown) or basal association between AMPK, p-LKB1(Ser428), p-ERK(Thr202/Tyr204) or total ERK in OKER cells (Fig.2C), these data indicate that ERK pathway activation could promote cell survival mediated by p-LKB1(Ser428) either in cells harboring WT or mutant $BRAF^{V600E}$.

p90RSK and PKA-mediated regulation of p-LKB1(Ser428)

There are increasing evidence that implicate another two kinases, p90RSK and the cyclic AMP-dependent protein kinase or protein kinase A (PKA), in the directly regulation of p-LKB1(Ser428) *in vivo* (14, 15). To investigate the possible implication of these kinases in the regulation of LKB1, OKER cells were treated with a specific p90RSK inhibitor, BI-D1870, resulting in almost complete ablation of p-LKB1(Ser428) (Fig.2D), no changes in p-ERK(Thr202/Tyr204) and slight increase in p-AMPKα(Thr172). Moreover, the interaction between p90RSK and LKB1 proteins was confirmed by immunoprecipitation (Fig.2F), supporting the possible direct role of p90RSK in the regulation of p-LKB1(Ser428) in OKER cells.

In addition, the contribution of PKA to the regulation of LKB1 activation was explored in the OKER cells. OKER cells showed increased levels of the allosteric activator of PKA, cAMP, compared to WT hepatocytes (27.0±3.4 and 2.7±0.1fmol/μg protein respectively, $p<0.05$). Treatment with H89, PKA inhibitor, decreased p-LKB1(Ser428) but had no effect on p-ERK(Thr202/Tyr204) and p-p90RSK(Thr359/Ser363) (Fig.2E), suggesting a PKA-mediated control of p-LKB1(Ser428) independently of the MEK/ERK pathway. No protein interaction between both kinases and the active p-PKAc(Thr197) was detected (Fig.2F). Furthermore, PKA has been reported to exert a negative effect on AMPK activity by phosphorylation (Ser485) (16). This evidence correlated with a slight increase in p-AMPKα(Thr172) combined with a reduction in p-AMPKα(Ser485) observed in H89-treated cells (Fig.2E).

Taken together, these data may suggest a possible influence of PKA in the LKB1-AMPK axis, regulating both the activation of LKB1(Ser428) and the inhibition of AMPK through p-AMPKα(Ser485).

Inhibition of DNA methylation blocks the Ras pathway and promotes apoptosis

We have previously shown that the deficiency in GNMT is closely linked to an epigenetic regulation in HCC development (6). 5-azacytidine inhibits DNA methyltransferase 1 (DNMT1), the major enzyme responsible for the maintenance of DNA methylation patterns during replication (17). In OKER cells, the levels of DNMT1 and 2 were statistically upregulated versus GNMT-WT and GNMT-KO hepatocytes (Suppl. Fig.2A). Moreover, the activity of DNMT was exclusively responsive to the 5-azacytidine treatment in OKER cells after 12 hours. Longer exposures rendered a regulation in GNMT-KO hepatocytes while WT were insensitive and OKER cells underwent apoptosis (Suppl. Fig.2B, C). Accordingly, the treatment of these cells with the demethylating drug re-established the expression of *SOCS* and *RASSF* inhibitors (Fig.3A) while no regulation was detected in WT hepatocytes. Finally, 5′-azacytidine treatment resulted in a clear inhibition of the Ras-GTP activity in OKER cells (Fig.3B). This effect correlated with a slight decrease in p-ERK(Thr202/Tyr204), p-p90RSK(Thr359/Ser363), p-LKB1(Ser428) and increased in p-AMPKα(Thr172) and a robust PARP cleavage in OKER cells as well as in GNMT-KO hepatocytes (Fig.3C, D). The apoptotic response to 5'-azacytidine in OKER cells was mediated by the mitochondrial pathway as detected by the increased of cytochrome c release to the cytosol (Fig.3C), the decrease of the anti-apoptotic protein Bcl-2 (Fig.3E) and the responsiveness of the cells to the drug after the ablation of Bcl-2 (Fig.3E).

Role of LKB1 and AMPK kinases in the apoptosis induced by 5'-azacytidine

In order to establish a causal link among the inhibition of LKB1 signaling and the AMPK reactivation, we knockdown AMPKα1 in OKER cells and investigate the apoptotic response after 5'-azacytidine treatment. As showed in Fig.4A and Suppl. Fig.3A right panel, the inhibition of AMPK signaling reduce PARP cleavage, whereas LKB1 deficiency slightly induced PARP cleavage under basal conditions that increased after 5′-azacytidine treatment (Fig.4B and Suppl. Fig.3A left panel). In addition, kinase-dead (KD)-LKB1(K78I) increased caspase-3 cleavage(Asp175) (Suppl. Fig.3B right and left panel). This effect is not restrictive to OKER cells, other hepatoma and hepatoblastoma cell lines like Huh7 and HepG2 with high levels of p-LKB1(Ser418), p-ERK(Thr202/Tyr204) and RAS showed an increased of caspase-3 activity after LKB1 ablation associated with an induction of p-AMPKα(Thr172) (Suppl. Fig.3C, D). Therefore, LKB1 overexpression revealed an upregulation of cell cycle proliferation markers (Suppl. Fig.3E). In contrast, in PLC cells, the modulation of LKB1 levels exerted no effect either on apoptosis or proliferation (Suppl. Fig.3C, D, E).

Finally, *GNMT* overexpression in these cell lines caused a significant increase in apoptosis and AMPK activity (Suppl. Fig.3F).

CaMKKβ as the upstream kinase of AMPK

OKER cells present LKB1 and AMPK misconnection. Interestingly, the re-activation of AMPK induces an apoptotic response in an independent manner of LKB1 activation. Other kinases have been reported to mediate AMPK activation, including the Ca^{++}/calmodulin-dependent protein kinase kinases (CaMKKs) (18, 19). STO-609, specific inhibitor of CaMKK, significantly decreased 5′-azacytidine-induced apoptosis and prevented AMPKα activation (Fig.4C), suggesting that CaMKK may play a role as the upstream kinase of AMPK in the OKER cells. pcDNA3-Flag-CaMKKα or pcDNA3-Flag-CaMKKβ transfection increased caspase-3 cleavage(Asp175) upon 5′-azacytidine treatment (Fig.4D).

Besides that, CaMKKβ induced p-AMPKα(Thr172) even under unstimulating conditions (Fig.4D and Suppl. Fig.4A). Moreover, CaMKKβ-ablation decreased p-AMPKα(Thr172) after 5′-azacytidine treatment (Fig.4E and Suppl. Fig.4B). Taken together, these results indicate that CaMKKβ may be the upstream kinase responsible for AMPK regulation in OKER cells.

Interestingly, it has been reported that PKA negatively regulates CaMKK activity (19). We have previously observed elevated levels of cAMP and PKA responsiveness for AMPK inactivation in OKER cells. While 5′-azacytidine reduced by 38% the intracellular levels of cAMP at 24 hours and induced apoptosis (Fig.4F), forskolin, a PKA activator, prevented this effect, recovering p-AMPKα(Ser485) inhibition and decreasing p-AMPKα(Thr172) activation (Fig.4F and Suppl. Fig.4C), suggesting the implication of the cAMP-PKA and CAMKK mediated pathway in the regulation of AMPK activity in OKER cells.

5′-azacytidine blocks tumor growth *in vivo*

To evaluate the direct therapeutic effect of 5′-azacytidine in the tumor progression *in vivo*, OKER cells were transfected with pBABE-puro-GFP vector and injected into the flanks of immune-deficient mice. Nine days after inoculation, 100% of mice developed solid tumors. Mice were randomly divided into control and 5′-azacytidine-treated groups and tumor progression was followed. We observed that 5′-azacytidine-treated group had lower tumor size than untreated mice ($0.479\pm0.086 cm^3$ and $0.941\pm0.139 cm^3$, respectively, $p<0.05$) (Fig. 5A). Histological analysis of the tumors revealed increased cell death (81.77%, $p<0.05$), decreased neo-angiogenesis (49.5%, $p<0.05$) and increased DNA fragmentation (69.1%, $p<0.05$) in 5′-azacytidine-treated mice compared to controls group (Fig.5B). 5′-azacytidine caused an 85.5% reduction in Ras activity and p-c-Raf(Ser338) ($p<0.05$) (Fig.5C and 5D). The histological examination and Western blot analysis of the tumors revealed decreased p-LKB1(Ser428) staining (70.5%), induction of p-AMPKα(Thr172) in the apoptotic areas, 79.2% increase ($p<0.05$) in p-p53(Ser15) together with increased expression of the p53 target, Bax (Fig.5F) and a decrease of Bcl-2 in the membrane fraction (Fig.5E and 5F). These results indicate that 5′-azacytidine mediates the inhibition of the tumor progression *in vivo*, in part through Ras inhibition, the inactivation of p-LKB1(Ser428), and the induction of AMPK and p53 proteins.

In vivo LKB1 silencing blocks tumor progression

The therapeutic effect of LKB1 ablation in the tumor progression was evaluated *in vivo*. Fifteen nude mice were injected subcutaneously with OKER-GFP cells. By day 3, all mice developed visible tumors and were assigned to three different experimental groups: injected intraperitoneally with (i)control siRNA; (ii)LKB1 siRNA; and with (iii)siRNA LKB1 and 5`-azacytidine (1mg/kg). LKB1 immunohistochemical analysis in the tumors revealed a significant decrease in LKB1 protein in both siRNA LKB1 groups, confirming the efficiency of the *in vivo* silencing assay (data not shown). At day six post-treatment, a $61.3\pm5.13\%$ reduction ($p<0.05$) in tumor growth was observed in LKB1 ablated tumors compared to control tumors (Fig.6A). This decrease was maintained until the end of the experimentation. Additionally, a significant reduction in both size and tumor weight measured at the end of the study were observed in both siRNA LKB1 groups compared to control tumors (Fig.6B and 6C).

Hematoxylin&eosin staining showed a significantly increased parenchyma disruption in both siRNA LKB1 groups (Fig.6D). These results correlated with the reduction in proliferating marker Ki-67 (31.2% and 44.7% siLKB1 and siLKB1+5`-azacytidine vs. control, respectively $p<0.05$) (Fig.6D) and neoangiogenic marker CD31 (Fig.6D).

In vivo LKB1 ablation also promoted a significant decrease of p-LKB1(Ser428) in non-necrotic areas and in apoptotic tissue in both siRNA LKB1 groups (Fig.6D). These results correlated with the induction of p-AMPKα(Thr172) and p-p53(Ser15) in both siRNA LKB1 groups (Fig.6D). This response suggested that *in vivo* ablation of LKB1 inhibited the tumor progression through a mechanism that implies the induction of AMPK and potentially p53-mediated tumor growth arrest.

Finally, *in vivo* LKB1 silencing significantly decreased Ras activity and p-c-Raf(Ser338) in the tumors (Fig.6E and 6F), and the combination with 5`-azacytidine improved the effect of LKB1 silencing up to ~97%. Similar results were obtained in OKER cells after LKB1 silencing (Suppl. Fig.5A), showing for the first time that LKB1, a bona fide tumor suppressor, regulates positively the activity of Ras, one of the major oncogenes involved in development and progression of human cancers.

Gene expression arrays were performed to compare tumors from control and LKB1 siRNA groups. The preliminary analysis revealed that genes encoding for mitochondrial apoptosis were highly represented, such as *APAF-1, BIM* and *CASPASE-6,* compared to non-silenced tumors (Suppl. Table 2 and Array Express accession: E-MEXP-3403). Additionally, upregulation of the *BCL2L1* gene was detected in LKB1 ablated tumors, while *BAD* was significantly downregulated in LKB1 siRNA tumors (Suppl. Table 2). In order to validate the results obtained in relation to LKB1-mediated Ras activity, we investigated the possible candidate genes involved in this process. The gene expression profile revealed that *in vivo* LKB1 ablation downregulated ~2.6 fold the expression of the *RASGRP3* gene (Suppl. Table 2), which encodes for a protein of the Ras family functioning as a Ras activator. Moreover, LKB1 silencing in the OKER cells decreased *RASGRP3* expression levels, RAS activity and p-c-Raf Ser338, confirming the results obtained *in vivo* (Suppl. Fig.5B). Furthermore the silencing of RASGRP3 in the OKER cells decreased cyclin D1 (data not shown) and increased the response in late apoptosis as detected by FACS analysis revealing the significance of this RAS-GTPase protein in OKER cell growth (Suppl. Fig.5C and 4D). Finally, a robust over-expression of *RASAL1* (3.59 fold), *RASA1* (3.61 fold), *RASA2* (2.44 fold), and *NF1* (2.04 fold) RAS GAPs was detected in LKB1 siRNA tumors. In HCC cells, reactivation of *RASAL1*, *RASA1–4*, *DAB2IP*, and *PITX1* inhibited proliferation, induced apoptosis, and suppressed Ras signaling in the presence of non-mutated RAS (20). Thus, this coordinated response mediated by the ablation of LKB1 gene could justify the inactivation of Ras activity in these tumors.

Alteration of the GNMT/LKB1/RASGRP3 axis is associated with poor prognosis in human HCC

Published microarrays obtained from an ONCOMINE search (http://www.oncomine.org) revealed in a cohort of 225 HCC human samples and 200 controls a statistically correlation between *GNMT* and *RASGRP3* gene expression (Fig.7A and B). Moreover, a statistical correlation was identified between *GNMT* and *STK11* levels in HCC (Fig.7C and 7D). Logistic regression was performed to quantify the predictability of a model with both genes (Fig Suppl. Fig.6B). The model shows a good predictability with an AUC of 0.782 (CI: 0.656–0.906) and AUC cross-validated of 0.731 (CI:0.590–0.870).

Finally, Western blot analyses of healthy *versus* surrounding and cancerous liver revealed a clear inverse correlation between the levels of GNMT and RASGRP3, p-LKB1(Ser428) and Ras-GTP activity (Fig.7E). Of note, tumors with poorer prognosis have the lowest levels of GNMT and p-AMPKα(Thr172) and the highest levels of p-LKB1(Ser428) and Ras-GTP ($p<0.05$) (Suppl. Table 3 and Suppl. Fig.6A), indicating that low GNMT levels and upregulated LKB1(Ser428), RASGRP3, and Ras activity might represent important prognostic markers for human HCC.

Discussion

Mounting evidence assigns an essential role for GNMT in liver health. GNMT is expressed in the liver, pancreas, and prostate (21), down-regulated in cirrhotic patients, and almost completely suppressed in HCC (22). Thus, *GNMT* has been proposed to be a tumor-susceptibility gene for liver cancer (23). GNMT-KO mice spontaneously develop steatosis, fibrosis, and HCC (6). An increase in hepatic SAMe leads to global DNA hyper-methylation and subsequent gene silencing of Ras inhibitors, with resulting hyper-activation of the Ras cascade in these mice (6). The Ras pathway is universally activated in human HCC (24).

In the current work, a new HCC cell line derived from GNMT-KO tumors, OKER cells, has been isolated, to investigate the proliferation of liver tumors characterized by a deficiency in *GNMT*, a chronic excess of SAMe and hyperphosphorylated LKB1(Ser428) (results are schematized in Suppl. Fig.7). To this respect, decreased expression of RAS inhibitors was observed in OKER cells, revealing that SAMe chronic excess may induce the Ras pathway hyperactivation. In fact, the non-mutated and hyperactivated Ras pathway regulates p-LKB1(Ser428) through ERK/p90RSK in the GNMT-KO derived tumor cells. A misconnection between LKB1 and AMPK was detected in OKER cells. In human melanoma, a hyperactivation of RAS, due to a mutation in $BRAF^{V600E}$, induced MEK/ERK/p90RSK-dependent LKB1 phosphorylation and LKB1-AMPK misconnection (9, 10). In the OKER cell line, the selective blockade of MEK1/2 and its target p90RSK reduced p-LKB1(Ser428) and induced p-AMPKα(Thr172), triggering apoptosis. While in WT hepatocytes LKB1 is the kinase upstream of AMPK, in OKER cells CaMKKβ is the kinase responsible for AMPK activation after a demethylated treatment in an independent manner of Ca^{++} signaling and under the negative control of PKA.

Altogether, these observations emphasize the regulation of p-LKB1(Ser428) by a non-mutated Ras pathway and suggest that suppression of GNMT in HCC acts as a driving force for Ras activation.

Demethylating agents have been widely used in liquid tumors (25). Taking into consideration the previous results of a strong reversion of GNMT-KO phenotype after nicotinamide treatment, OKER cells were stimulated with 5`-azacytidine (26). OKER cells and GNMT KO hepatocytes were more responsive to inhibition of DNMT after 5'-azacytidine, while WT hepatocytes were insensitive to this effect. This data highlighted the potential use of demethylating agents as a drug targeting in HCC with low GNMT and high DNMT levels. Hence, both genes may play a critical role in the malignant progression of HCC (27). Moreover, 5′-azacytidine re-expressed the RAS inhibitors, decreased Ras activity, and downregulated the phosphorylation of the ERK/p90RSK/LKB1 cascade, leading to AMPK activation and apoptosis. A similar response was detected in primary hepatocytes isolated from 3-month-old GNMT-KO mice. Furthermore, the overexpression of *GNMT* sensitized OKER cells to 5′-azacytidine, increasing apoptosis (data not shown). AMPKα1 silencing in OKER cells prevented significantly 5'-azacytidine-mediated apoptosis, substantiating an apoptotic mediator role of AMPK. Interestingly, AMPK has been described to directly activate p53(Ser15) (28), and treatment with 5'-azacytidine induced nuclear p-p53(Ser15) in OKER cells, strengthening the p53 cascade as a possible executor of the AMPK-mediated apoptosis (data not shown).,

Furthermore, the anti-tumor properties of 5`-azacytidine observed *in vitro* were validated in a xenograft tumor model in nude mice revealing a decreased tumor growth, increased cell death, reduced Ras activity and p-LKB1(Ser428), and activating AMPKα(Thr172) and p53(Ser15) in treated tumors, highlighting the importance of the RAS/LKB1/AMPK axis and epigenetic mechanisms during HCC development.

In OKER cells, CaMKKβ is the kinase responsible for AMPK activation as previously described in LKB1-deficient cells (18,19). However, this mechanism was Ca^{++}-independent (18), as the Ca^{++}-chelating compound, BAPTA-AM, did not prevent either 5′-azacytidine-mediated AMPK activation or apoptosis (data not shown). An alternative mechanism to Ca^{++} involves PKA-mediated inhibitory phosphorylation of CaMKK (29). OKER cells presented elevated levels of cAMP, the allosteric regulator of PKA activity. At the same time, PKA inactivates AMPK by phosphorylation at Ser485, opening the possibility of the cAMP/PKA pathway as the mediator of the CaMKK-AMPK axis. In this regard, 5`-azacytidine decreased the intracellular cAMP and the adenyl cyclase activator, forskolin, which raised the intracellular cAMP, prevented 5`-azacytidine-mediated AMPK activation and PARP cleavage, thus reinforcing the implication of the cAMP signaling pathway in the regulation of AMPK activation and apoptosis in OKER cells.

The function of LKB1 was assessed in OKER cells, where LKB1-deficiency induced a slight increase in PARP cleavage under unstimulating conditions and sensitized even more the OKER cells to 5′-azacytidine. Moreover, kinase-dead LKB1 induced apoptosis in the OKER cells, reinforcing the essential contribution of LKB1 in the survival signaling. Finally, LKB1 silencing in OKER cells decreased Ras activity, in addition, to inhibit c-Raf (Ser338) directly related with cell proliferation, survival, and tumorigenesis (30). These results highlighted the undefined crosstalk between LKB1 and the oncogene RAS. The effect was not exclusive to OKER cells. In HepG2 and Huh7 where LKB1 was phosphorylated (Ser428), its knockdown induced apoptosis, while PLC cells were insensitive. This data pointed out that the differential response observed could potentially be due to the basal LKB1(Ser428) levels of each cell. Accordingly, similar outcome was obtained after GNMT overexpression in this hepatoma cells, suggesting a close correlation of this tumor suppressor with the presence of LKB1(Ser428) hyperphosphorylation. The relevance of these findings was further substantiated through *in vivo* silencing of LKB1 in the xenograft model of OKER cells in nude mice, where LKB1 ablation decreased the tumor growth, Ras activity and increased necrosis, p-AMPKα(Thr172), and p-p53(Ser15). The gene expression pattern of LKB1-ablated tumors revealed a downregulation of the RASGRP3 gene, which activates Ras by maintaining its GTP-bound state (31). This might explain the inactivation of Ras activity in LKB1-deficient tumors, opening a new field of investigation regarding the crosstalk between LKB1 and RAS. Additionally, RASGRP3 silencing induced apoptosis, confirming its importance in OKER cells growth.

In human HCC, an inverse correlation was detected between the levels of *GNMT* and p-AMPKα(Thr172) and those of p-LKB1(Ser428), RASGRP3, and Ras activity, implying that downregulation of GNMT and AMPK is associated with activation of the Ras/LKB1/RASGRP3 axis and the poorest prognosis of the disease. Moreover, the ROC curve analysis that was used to assess the potential of *GNMT* and *STK11* levels in HCC diagnosis showed a good predictive model. Hence, the present data indicate that activation of the RAS/LKB1/RASGRP3 cascade might possess an important prognostic role in human liver cancer, being the first report correlating LKB1 and Ras activity in a context of HCC with low *GNMT* expression. Furthermore, these findings open the possibility to design new therapeutic strategies for the treatment of liver cancer.

Methods

Cell lines

A broad description of OKER cells isolation after collagenase digestion of tumor specimens from HCC of GNMT-KO mice (6), primary mouse hepatocytes purification and cell culture is provided in Supplemental Material and Methods. All procedures performed in mice were done following the institutional guidelines of laboratory animal use.

Drug Treatments

Described in Supplemental Material Table S4 and References.

Antibody description

Summarized in Table S5.

Sequence of primers used for RT-PCR analysis

Described in Table S6.

5′-azacytidine treatment

OKER-GFP cells (OKER-pBABE-puro-GFP) were injected subcutaneously into the lumbar regions of 10 female athymic C57BL/6J nude mice. 5′-azacytidine was administered intraperitoneally daily at 1mg/kg dose for 13 days. Tumor volume ((lengthxwidth^2)/2) was measured.

In vitro silencing

Oligonucleotides sequences used for gene silencing assays were provided in Table S7.

In vivo LKB1 silencing

OKER-GFP cells were injected into 15 male athymic C57BL/6J nude mice, as previously described. Three days after cell inoculation, animals were divided into 3 experimental groups: (i)siControl, (ii)siLKB1 and (iii)siLKB1+5′-azacytidine, 50μM-siRNA dose were intraperitoneally injected using jetPEI (Polyplus) following manufacturer's instructions. 5′-azacytidine treatment was daily administered and silencing assays were done every 3 days.

Gene expression arrays

Three RNA samples from OKER cells and primary WT mouse hepatocytes (3 months old) were hybridized to MouseWG-6 v2.0 Expression BeadChips (Illumina Inc) analyzed with the R/Bioconductor statistical computing environment (www.r-project.org, www.bioconductor.org). Four samples of siControl and siLKB1 from the xenograft model in nude mice were analyzed. Microarray analysis description is provided in Supplemental Material and Methods. Published microarrays obtained from an ONCOMINE search were used to check in an independent manner the possible existence of correlation of *GNMT* and *RASGRP3* gene expression. All computations were done using R statistical software.

Predictive modeling of HCCB and HCCP status using *GNMT* and *STK11* signature

Logistic regression was performed to quantify the predictability of a *GNMT* and *STK11* model. In the absence of an independent set, we evaluated the performance of the model using leave-one-out cross-validation (LOOCV). ROC related computation was performed using DiagnosisMed (http://CRAN.R-project.org/package=DiagnosisMed) and pROC package.24. All computations were performed using R software.

Human Samples

Described in Suppl.Table 2. Institutional Review Board approval was obtained at participating hospitals and the National Institutes of Health.

Immunohistochemistry

Immunohistochemistry of formalin-fixed, paraffin-embedded liver sample sections were performed as described (8). Images were taken with a 100× objective from an

epifluorescence microscope AXIO Imager.D1 (Zeiss). Apoptosis was analyzed with the In situ Cell Death Detection Kit (Roche) following manufacturer's instructions.

Gene sequencing

Described in Suppl.Table 1.

Cell transfection

FLAG-CaMKKalpha and beta were gifted by Thomas R Soderling.

Immunoprecipitation experiments

500μg of whole-cell proteins were immunoprecipitated overnight at 4°C with 10μg of p-LKB1(Ser428) or AMPKα1 antibodies, and protein A-Sepharose beads (SIGMA). IgG1 (BD Pharmingen) was used as negative control.

cAMP measurement

cAMP was measured as described in the Biotrak enzyme immunoassay (EIA) system (Amersham Biosciences, UK).

SAMe measurements

Intracellular SAMe levels were measured as described previously (7).

Statistical analysis

All experiments were performed in triplicate. Data expressed as mean±SEM. Statistical significance was estimated with Student's *t* test. A pvalue<0.05 was considered significant.

Supplementary Material

Refer to Web version on PubMed Central for supplementary material.

Acknowledgments

Financial Support: This work is supported by grants from NIH AT-1576 and NIH AT-004896 (to S.C.L., M.L.M-C. and J.M.M.), SAF 2011-29851 (to J.M.M), ETORTEK-2010 (to M.L.M.-C), Sanidad Gobierno Vasco 2008 and Educación Gobierno Vasco 2011 (to M.L.M.-C), FIS PI11/01588 (to M.L.M.-C), Sanidad Gobierno Vasco 2012 (to MVR), Educación Gobierno Vasco (to J.M.M.), FIS PS09/02010 and Program Ramón y Cajal (to N.B), Deutsche Forschungsgemeinschaft DFG (grant number Ev168/2-1 to M.E), and NIH DK15289 and DK180010 (to C.W). Ciberehd is funded by the Instituto de Salud Carlos III.

References

1. Thorgeirsson SS, Grisham JW. Molecular pathogenesis of human hepatocellular carcinoma. Nat Genet. 2002; 31:339–46. [PubMed: 12149612]
2. Mato JM, Martinez-Chantar ML, Lu SC. Methionine metabolism and liver disease. Annu Rev Nutr. 2008; 28:273–93. [PubMed: 18331185]
3. Martinez-Chantar ML, Vazquez-Chantada M, Garnacho M, et al. S-adenosylmethionine regulates cytoplasmic HuR via AMP-activated kinase. Gastroenterology. 2006; 131:223–32. [PubMed: 16831604]
4. Lu SC, Alvarez L, Huang ZZ, Chen L, et al. Methionine adenosyltransferase 1A knockout mice are predisposed to liver injury and exhibit increased expression of genes involved in proliferation. Proc Natl Acad Sci U S A. 2001; 98:5560–5. [PubMed: 11320206]

5. Martinez-Chantar ML, Corrales FJ, Martinez-Cruz LA, et al. Spontaneous oxidative stress and liver tumors in mice lacking methionine adenosyltransferase 1A. Faseb J. 2002; 16:1292–4. [PubMed: 12060674]
6. Martínez-Chantar ML, Vázquez-Chantada M, Ariz U, et al. Loss of the glycine N-methyltransferase gene leads to steatosis and hepatocellular carcinoma in mice. Hepatol. 2008; 47:1191–9.
7. Huynh H, Nguyen TT, Chow KH, et al. Over-expression of the mitogen-activated protein kinase (MAPK) kinase (MEK)-MAPK in hepatocellular carcinoma: its role in tumor progression and apoptosis. BMC Gastroenterol. 2003; 3:19. [PubMed: 12906713]
8. Newell P, Toffanin S, Villanueva A, et al. Ras pathway activation in hepatocellular carcinoma and anti-tumoral effect of combined sorafenib and rapamycin in vivo. J Hepatol. 2009; 51:725–33. [PubMed: 19665249]
9. Zheng B, Jeong JH, Asara JM, et al. Oncogenic B-RAF negatively regulates the tumor suppressor LKB1 to promote melanoma cell proliferation. Mol Cell. 2009; 33:237–47. [PubMed: 19187764]
10. Esteve-Puig R, Canals F, Colomé N, et al. Uncoupling of the LKB1-AMPK alpha energy sensor pathway by growth factors and oncogenic BRAF. PLoS One. 2009; 4:e4771. [PubMed: 19274086]
11. Vázquez-Chantada M, Ariz U, Varela-Rey M, et al. Evidence for LKB1/AMP-activated protein kinase/ endothelial nitric oxide synthase cascade regulated by hepatocyte growth factor, S-adenosylmethionine, and nitric oxide in hepatocyte proliferation. Hepatology. 2009; 49:608–17. [PubMed: 19177591]
12. Martínez-López N, Varela-Rey M, Fernández-Ramos D, et al. Activation of LKB1-Akt pathway independent of phosphoinositide 3-kinase plays a critical role in the proliferation of hepatocellular carcinoma from nonalcoholic steatohepatitis. Hepatology. 2010; 52:1621–31. [PubMed: 20815019]
13. Llovet JM, Ricci S, Mazzaferro V, Hilgard P. Sorafenib in advanced hepatocellular carcinoma. N Engl J Med. Jul 24; 2008 359(4):378–90. [PubMed: 18650514]
14. Sapkota GP, Kieloch A, Lizcano JM, et al. Phosphorylation of the protein kinase mutated in Peutz-Jeghers cancer syndrome, LKB1/STK11, at Ser431 by p90(RSK) and cAMP-dependent protein kinase, but not its farnesylation at Cys(433), is essential for LKB1 to suppress cell growth. J Biol Chem. 2001; 276:19469–82. [PubMed: 11297520]
15. Collins SP, Reoma JL, Gamm DM, et al. LKB1, a novel serine/threonine protein kinase and potential tumour suppressor, is phosphorylated by cAMP-dependent protein kinase (PKA) and prenylated in vivo. Biochem J. 2000; 345:673–80. [PubMed: 10642527]
16. Hurley RL, Barré LK, Wood SD, et al. Regulaton of AMP-activated protein kinase by multisite phosphorylation in response to agents that elevate cellular cAMP. J. Biol CHem. 2006; 281:36662–72. [PubMed: 17023420]
17. Spada F, Haemmer A, Kuch D, et al. DNMT1 but not its interaction with the replication machinery is required for maintenance of DNA methylation in human cells. J Cell Biol. 2007; 176:565–71. [PubMed: 17312023]
18. Hawley SA, Pan DA, Mustard KJ, et al. Calmodulin-dependent protein kinase kinase-beta is an alternative upstream kinase for AMP-activated protein kinase. Cell Metab. 2005; 2:9–19. [PubMed: 16054095]
19. Hurley RL, Anderson KA, Franzone JM, et al. The Ca2+/calmodulin-dependent protein kinase kinases are AMP-activated protein kinase kinases. J Biol Chem. 2005; 280:29060–6. [PubMed: 15980064]
20. Wayman GA, Tokumitsu H, Soderling TR. Inhibitory cross-talk by cAMP kinase on the calmodulin-dependent protein kinase cascade. J Biol Chem. Jun 27; 1997 272(26):16073–6. [PubMed: 9195898]
21. Calvisi DF, Ladu S, Conner EA, et al. Inactivation of Ras GTPase-activating proteins promotes unrestrained activity of wild-type Ras in human liver cancer. J Hepatol. 2011; 54:311–9. [PubMed: 21067840]
22. Ogawa H, Fujikoa M. Purification and properties of glycine N-methyltransferase from rat liver. J Biol Chem. 1982; 257:3447–3452. [PubMed: 6801046]

23. Avila MA, Berasain C, Torres L, Martín-Duce A, et al. Reduced mRNA abundance of the main enzymes involved in methionine metabolism in human liver cirrhosis and hepatocellular carcinoma. J Hepatol. 2000; 33:907–914. [PubMed: 11131452]
24. Calvisi DF, Ladu S, Gorden A, et al. Ubiquitous activation of Ras and Jak/Stat pathways in human HCC. Gastroenterology. Apr; 2006 130(4):1117–28. [PubMed: 16618406]
25. Hirasawa Y, Arai M, Imazeki F, et al. Methylation status of genes upregulated by demethylating agent 5-aza-2'-deoxycytidine in hepatocellular carcinoma. Oncology. 2006; 71:77–85. [PubMed: 17341888]
26. Varela-Rey M, Martínez-López N, Fernández-Ramos D, et al. Fatty liver and fibrosis in glycine N-methyltransferase knockout mice is prevented by nicotinamide. Hepatology. 2010; 52:105–14. [PubMed: 20578266]
27. Saito Y, Kanai Y, Nakagawa T, et al. Increased protein expression of DNA methyltransferase (DNMT) 1 is significantly correlated with the malignant potential and poor prognosis of human hepatocellular carcinomas. Int J Cancer. Jul 1; 2003 105(4):527–32. [PubMed: 12712445]
28. Jones RG, Plas DR, Kubek S, et al. AMP-activated protein kinase induces a p53-dependent metabolic checkpoint. Mol Cell. 2005; 18:283–93. [PubMed: 15866171]
29. Colomer J, Means AR. Physiological roles of the Ca2+/CaM-dependent protein kinase cascade in health and disease. Subcell Biochem. 2007; 45:169–214. [PubMed: 18193638]
30. Mielgo A, Seguin L, Huang M, Camargo MF, et al. A MEK-independent role for CRAF in mitosis and tumor progression. Nat Med. Nov 13; 2011 17(12):1641–5. [PubMed: 22081024]
31. Rebhun JF, Castro AF, Quilliam LA. Identification of guanine nucleotide exchange factors (GEFs) for the Rap1 GTPase. Regulation of MR-GEF by M-Ras-GTP interaction. J Biol Chem. Nov 10; 2000 275(45):34901–8. [PubMed: 10934204]

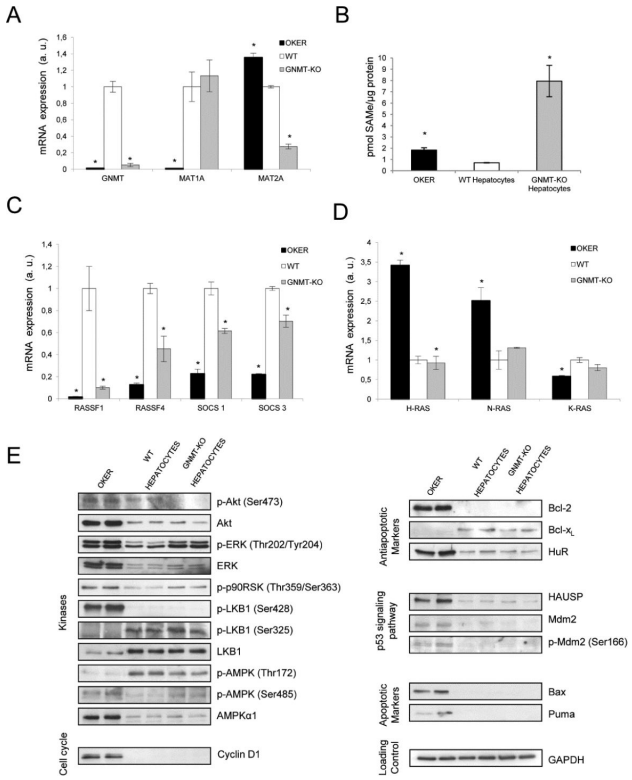

Figure 1. Characterization of OKER Cells

Graphical representation (mean±standard error of the mean [SEM]) of (A) mRNA expression (arbitrary units) of the indicated genes, *p<0.05 OKER and GNMT-KO hepatocytes versus -WT mouse hepatocytes. (B) intracellular levels of SAMe. *p<0.05, OKER and GNMT-KO hepatocytes versus -WT hepatocytes, and (C) and (D) mRNA expression (arbitrary units) of the indicated genes, *p<0.05 OKER and GNMT-KO hepatocytes versus -WT mouse hepatocytes. (E) Total protein extracts from OKER, GNMT-KO and -WT mouse hepatocytes were analyzed via Western blotting with the indicated antibodies.

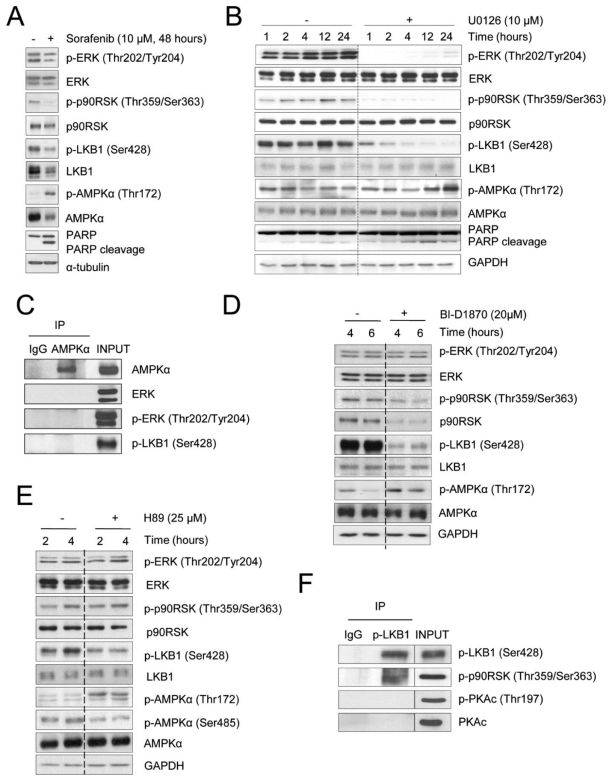

Figure 2. Ras/MEK/ERK-mediated p-LKB1(Ser428) regulation

(A) OKER cells were cultured with (A) sorafenib(10μM), (B) U0126(10μM), (D) BI-D1870(20μM), and (E) H89(25μM). Whole-cell lysates were analyzed via WB. The extracts were immunoprecipitated with (C) AMPKα1 or (F) p-LKB1(Ser428) antibodies. Immunoprecipates (IP) and lysates (INPUT) were analyzed via WB.

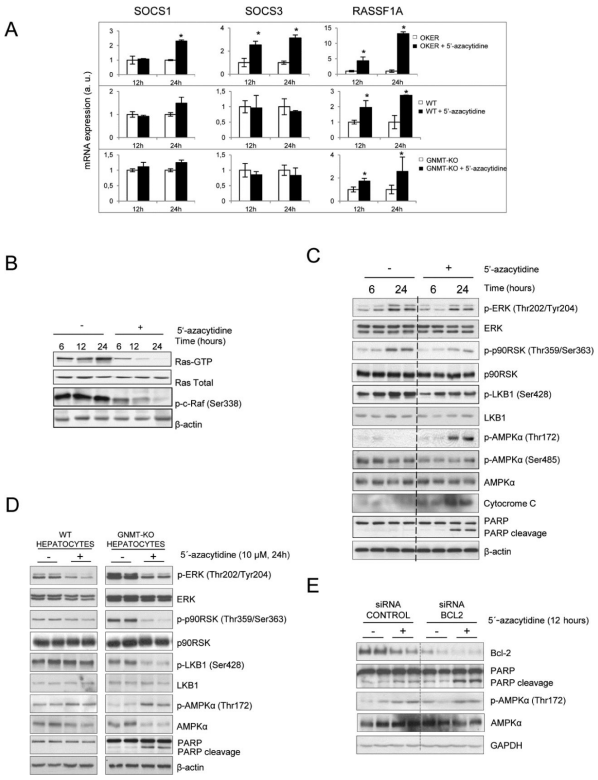

Figure 3. 5′-azacytidine inactivates the Ras pathway in OKER cells

OKER cells and GNMT-WT and -KO hepatocytes were treated with 5'-Azacytidine(10μM). (A) Graphical representation of the mRNA expression, *p<0.05 treated versus untreated cells. (B) Ras activity was assessed and probed with anti-RAS antibody. (C, D) Cytosolic and whole-cell extracts of OKER cells and GNMT-WT and -KO hepatocytes were analyzed via WB. (E) OKER cells transfected with Control or Bcl-2 siRNA and treated with 5′-azacytidine for 12 hours were analyzed by WB.

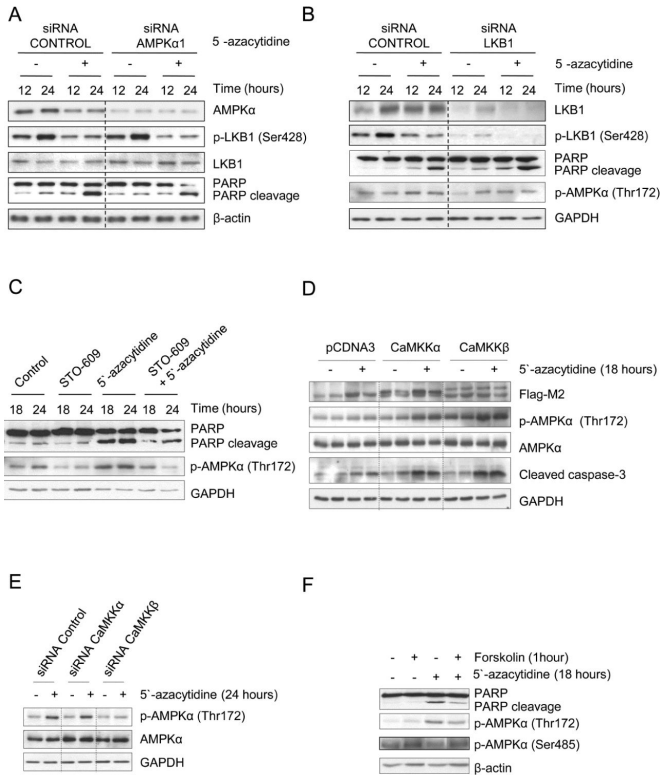

Figure 4. Influence of LKB1 and CaMKKβ-mediated AMPK response to 5'-Azacytidine in the OKER cells

OKER cells were transfected with Control (A) AMPKα1 or (B) LKB1 siRNA prior treatment with 10μM 5'-Azacytidine. Cell lysates were analyzed via WB. OKER cells were incubated with (C) STO-609(10μM) or (F) forskolin(10μM) for 1 hour before 5′-azacytidine treatment for the indicated times. OKER cells were transfected with (D) pcDNA3-Flag-CaMKKα or pcDNA3-Flag-CaMKKβ or (E) control, CAMKKα or CaMKKβ siRNAs and treated with 5′-azacytidine. Whole-cell lysates were analyzed via WB.

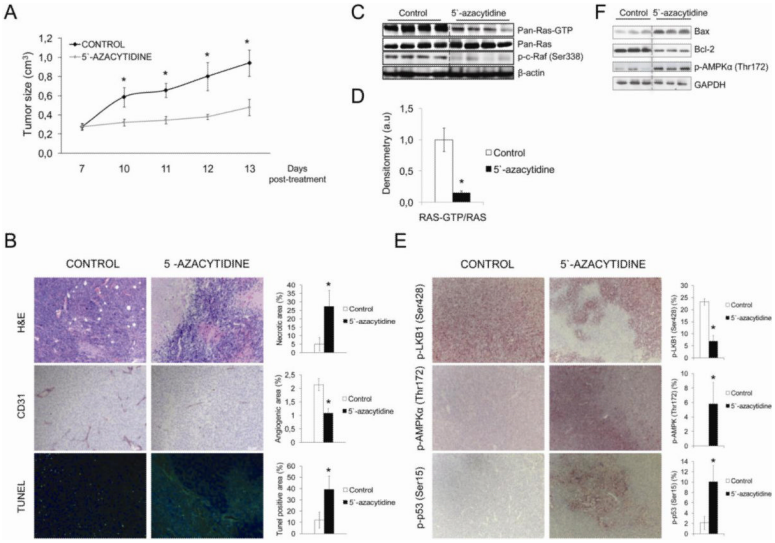

Figure 5. 5′-azacytidine attenuates tumor growth

2×10^6 OKER-GFP cells were injected subcutaneously as described in Methods section (A) Graphical representation of tumor volume. *p<0.05, 5′-azacytidine versus control. Paraffin-embedded tumor sections were stained with (B) hematoxylin&eosin, CD31 counterstained with hematoxylin and TUNEL assay, and (E) p-LKB1(Ser428), p-AMPKα(Thr172) and p-p53(Ser15) (left). Graphical representation of the quantitative analysis for each staining. *p<0.05, 5′-azacytidine versus control (right). Original magnification 200×. (C) Ras activity was assessed and probed with anti-RAS antibody (D). Fold change-graphical representation in the Ras activity. *p<0.05, 5′-azacytidine versus control. (F) Whole-tissue extracts from tumors were analyzed by WB.

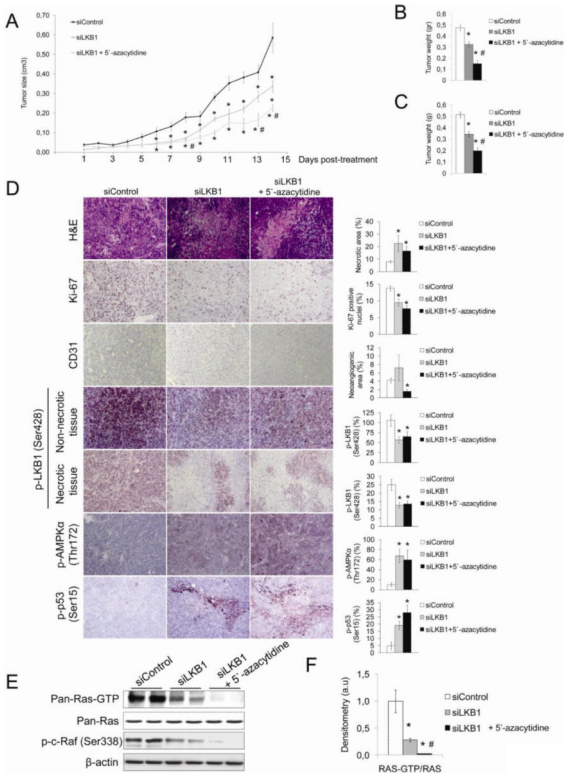

Figure 6. LKB1 ablation attenuates tumor growth

Graphical representation of (A) changes in tumor size, (B) tumor size increment and (C) tumor weight at the end of the experiment. *$p<0.05$ and $^{\#}p<0.05$ (siRNA LKB1, versus siRNA Control and siRNA LKB1+5′-azacytidine respectively. (D) Paraffin-embedded sections of tumors were stained with corresponding antibodies (left). Graphical representation of the quantitative analysis for each staining. *$p<0.05$ versus control siRNA (right). (E) Ras activity was assessed as described before. (F) Fold change-graphical representation in Ras activity (right), *$p<0.05$ siRNA LKB1 versus siRNA control. $^{\#}p<0.05$, siRNA LKB1 versus siRNA LKB1+5′-azacytidine.

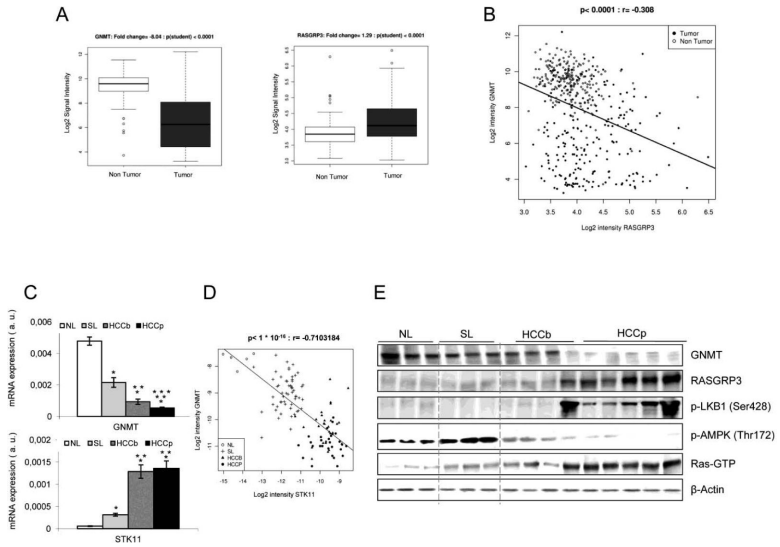

Figure 7. GNMT, LKB1 and Ras activity correlation

(A) Boxplots of *GNMT* (Fold change - 3.04:p(student)<0.0001) and *RASGRP3* (Fold change +1.29:p(student)<0.0001) levels in HCC (225 samples) and non-tumoral human samples(200). (B) Pearson correlation with (r)-0.308 and associated p-value<$1*10^{-11}$ between *GNMT* and *RASGRP3* genes. (C) Representation of *GNMT* and *STK11* expression levels in 29 HCCb and 27 HCCp. (D) Pearson correlation with (r)-0.71 and associated p-value<$1*10^{-16}$ between *GNMT* and *STK11* in the NL, SL, HCCb and HCCp. (E) Protein expression were analyzed via WB from the human samples at different states (NL=Normal Liver; SL=surrounding liver near the tumor; HCCb, Hepatocellular carcinoma with better prognosis; HCCp, Hepatocellular carcinoma with poor prognosis.